International Journal of Advanced Medical Sciences and Technology (IJAMST)
ISSN: 2582-7596 (Online), Volume-5 Issue-6, October 2025

Evaluate the Effects of Gamma Radiation (16 Sv/h), Neutron Radiation (3 Sv/h), and a Mixed Radiation Field on the Structural and Biophysical Properties of Bones

Mohamed S. Nasr Eldin, Ahmed. A Emara, Hala M. Ahmed

Abstract: ***Background:*** ***Ionizing radiation, including gamma and neutron radiation, can adversely affect bone structure, mineralization, and tissue integrity. While individual effects of gamma or neutron exposure have been studied, comparative analyses of their isolated and combined impacts on bone's structural and biophysical properties remain limited.*** ***Objective:*** ***This study aimed to evaluate the effects of gamma radiation (16 µSv/h), neutron radiation (3 µSv/h), and combined exposure on bone mineral content, collagen synthesis, cytokine levels, biomechanical properties, and histopathological changes in rats.*** ***Materials and Methods:*** ***Eighty male albino rats were divided into four groups: control (no radiation), gamma-exposed, neutron-exposed, and combined gamma-neutron exposure. Bone calcium was measured using atomic absorption spectrophotometry, and collagen content was quantified via hydroxyproline-based colourimetric assays. Serum interleukin-1β (IL-1β) and tumour necrosis factor-alpha (TNF-α) levels were determined using ELISA. Biomechanical properties of tibia bones, including tensile strength, stiffness, and energy absorption, were assessed through stress-strain analysis and cyclic loading. Skin and mammary tissues were examined histologically using hematoxylin and eosin staining.*** ***Results:*** ***Radiation exposure reduced calcium and collagen content, with the most pronounced effects observed in neutron and combined radiation groups. TNF-α levels were significantly elevated in irradiated rats, while IL-1β showed a non-significant upward trend, indicating an inflammatory response. Biomechanical analysis revealed reduced bone strength and increased energy dissipation, suggesting microstructural damage. Histological examination confirmed inflammation, necrosis, and impaired regenerative capacity, particularly in the combined radiation group.*** ***Conclusion:*** ***Gamma and neutron radiation, both individually and in combination, hurt bone mineralisation, collagen synthesis, inflammatory cytokine balance, and biomechanical integrity. These findings underscore the susceptibility of skeletal tissue to ionizing radiation and highlight the importance of protective strategies in clinical, occupational, and spaceflight environments. Future research should explore interventions targeting oxidative stress and inflammation to mitigate radiation-induced musculoskeletal damage.***

Keywords: Gamma Radiation; Neutron Radiation; Bone Biomechanics; Collagen; Calcium; Cytokines; Histopathology

Abbreviations:
AAS: Atomic Absorption Spectrophotometry;
ELISA: Enzyme-Linked Immunosorbent Assay;
H&E: Hematoxylin & Eosin;
IL-1β: Interleukin-1 Beta;
TNF-α: Tumor Necrosis Factor-Alpha

I. INTRODUCTION

Evaluation of the Effects of Gamma Rays and Neutrons on Bone Structural and Biophysical Properties Gamma radiation causes cellular damage primarily through the generation of high-energy electrons, with their kinetic energy determined by the incident photon energy within biological tissues. These electrons originate from three primary interactions: the photoelectric effect, Compton scattering, and pair creation. The specific interaction depends on the gamma photon energy [1]. Neutrons, initially characterized by high velocities, predominantly undergo scattering and capture interactions as they decelerate within tissues. Fast neutrons lose energy via scattering with light atoms such as hydrogen, carbon, nitrogen, and oxygen. As their energy decreases toward thermal levels, they become more likely to be captured by nuclei within the tissue [2]. When a neutron encounters tissue-equivalent material, it may either pass through unaffected or interact through elastic or inelastic scattering and absorption (capture). The elastic cross-section for primary tissue nuclei decreases with increasing neutron energy, influencing the probability of interactions [3]. During a head-on collision with a hydrogen nucleus, the neutron transfers its entire kinetic energy. In contrast, collisions with heavier nuclei transfer only a fraction, producing secondary ionising particles that deposit energy via excitation and ionisation processes. The mean free path of high-energy neutrons within tissue depends on the collision frequency and spatial distribution of nuclei [4].

The mechanical integrity of bone, its strength and stiffness, remains of significant interest due to its role as both a structural and biological material. Recent studies suggest that collagen's role

Manuscript received on 11 August 2025 | First Revised Manuscript received on 02 September 2025 | Second Revised Manuscript received on 17 September 2025 | Manuscript Accepted on 15 October 2025 | Manuscript published on 30 October 2025.
*Correspondence Author(s)
Dr. Mohamed S. Nasr Eldin, Department of Radiology and Medical Imaging, Faculty of Applied Health Sciences Technology, October 6 University, 6th of October City, Egypt, Email ID: mohamedsamieh.ams@o6u.edu.eg. ORCID ID: 0000-0002-9596-3816
Dr. Ahmed. A Emara, Department of Radiology and Medical Imaging, Faculty of Applied Health Sciences Technology, October 6 University, 6th of October City, Egypt, Email ID: Ahmedemara.ams@o6u.edu.eg, ORCID ID: 0009-0003-2661-2881
Prof. Dr. Hala M. Ahmed*, Department of Medical Biophysics: Biomedical Equipment, Faculty of Applied Health Sciences Technology, October 6 University, 6th of October City, Egypt. bakar_tarek_76@hotmail.com, ORCID ID: 0000-0001-5833-6744

in determining overall bone strength and stiffness may be limited, although it significantly influences the energy threshold required for matrix breakdown [5]. The modulus of toughness, a key fracture mechanics property, quantifies the energy absorption capacity before failure and is calculated as the area under the stress-strain curve. It can also be described as the stress intensity factor required to initiate crack propagation [6].

Figure 1 illustrates a load-deformation curve used to determine mechanical properties such as strength, stiffness, and energy absorption. The slope of the linear (elastic) region indicates stiffness, while the area under the curve up to failure reflects the work or energy capacity of the bone [7]. These properties are classified as extrinsic, influenced by tissue characteristics, bone size, and shape. Normalising these parameters to the cross-sectional area or moment of inertia yields stress-strain curves, which reveal the intrinsic material properties. The ultimate stress indicates the material's inherent strength, while the elastic modulus (slope of the stress-strain curve) reflects stiffness. The area under the stress-strain curve corresponds to the toughness modulus, which measures the energy required to cause failure, independent of bone size or shape [8].

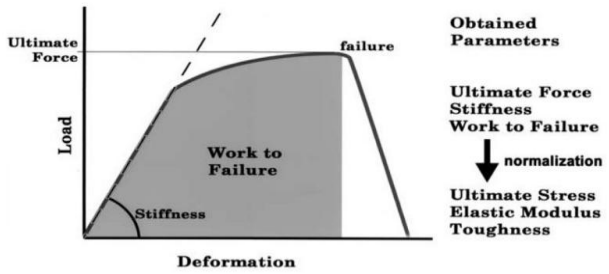

[Fig.1: Illustrates a Load-Deformation Curve that Enables the Measurement of Strength, Stiffness, and Work (Energy) until Failure]

A. The Aim of The Work

This study aims to evaluate the effects of gamma radiation (16 Sv/h) and neutron radiation (3 Sv/h), both individually and combined, on the structural and biophysical properties of bones. Additionally, the research will analyze histopathological changes in the skin across all experimental groups. The study will also measure biochemical markers, including calcium ion levels, collagen content, and cytokines (specifically IL-1 and TNF-α), to elucidate the biological impact of radiation exposure.

II. MATERIALS AND METHODS

A. Animal Cohorts

The present study utilized 80 male albino rats, each weighing between 100 and 120 grams, obtained from the National Research Centre, Dokki, Giza, Egypt. The animals were housed at the Animal Facility of the Zoology Department, Faculty of Science, Cairo University, under controlled environmental conditions (22–25°C) with a 12-hour light/dark cycle. They had unrestricted access to water and a standard pelleted diet. The experimental procedures adhered to the guidelines set forth by the International Commission on Radiological Protection (ICRP, 2024), ensuring radiation doses within acceptable safety limits. The experimental design is summarized in Table 1.

Table I: Presents the Details of the Experimental Design

Groups	Number of Animals	Radiation Exposure
A	20	No radiation.
B	20	Gamma radiation (16μSv/h).
C	20	Neutrons (3μSv/h).
D	20	Mixed (Gamma radiation (16μSv/h) & Neutrons (3μSv/h).

B. Gamma Radiation (16 μSv/h)

Gamma radiation was generated by Americium-241 (Am-241), with an average dose rate of approximately 16 μSv/h. Animals were housed within Perspex cages measuring 100×50×60 cm³, positioned 0.25 meters from the source. The cages were placed in front of the gamma source to ensure uniform exposure.

C. Neutron Radiation (3 μSv/h)

Neutron exposure was achieved using a neutron source, with an average dose rate of 3 μSv/h. Similar to gamma exposure, animals were confined within Perspex cages of identical dimensions and positioned 0.25 meters from the neutron source, ensuring consistent exposure conditions.

D. Combined Gamma and Neutron Radiation Exposure

Animals in this group were subjected to simultaneous gamma (16 μSv/h) and neutron (3 μSv/h) radiation within the same enclosure, maintaining equal distance from both sources for a defined exposure period.

E. Bone Calcium Concentration Measurement

Calcium levels in bone tissue were determined by first preparing bone ash after specimen extraction. Each specimen was weighed and dissolved in 10% nitric acid for 24 hours. Calcium content was quantified using atomic absorption spectrophotometry (AAS) [9]. The formation of a violet complex with o-cresolophthalein in an alkaline medium allowed spectrophotometric measurement at 560 nm, with calcium concentrations directly proportional to absorbance.

F. Bone Collagen Content

Bone collagen was quantified through a multi-step process. Soft tissues were removed from bones, which were then freeze-dried. The diaphyseal cortical bone segment (~15 mg) underwent demineralization in 0.5 M EDTA at 4°Cover 14 days. After incubation in PBS with iodoacetamide and EDTA, collagen was digested overnight at 37°C with 0.5 mg/mL chymotrypsin. Supernatants containing solubilised collagen were separated by centrifugation, hydrolysed in 6 M HCl at 110°C, dried, and reconstituted in borate buffer [10] [11]. Hydroxyproline content was measured colourimetrically via Chloramine-T and DMBA reagents, with collagen percentage calculated based on hydroxyproline levels relative to initial tissue content [12].

G. Serum Cytokine Levels (IL-1 and TNF-α)

Serum levels of interleukin-1 beta (IL-1β) and tumour necrosis factor-alpha (TNF-α) were quantified using enzyme-linked

immunosorbent assay (ELISA) kits (BD550788, BD Biosciences (2023), following the manufacturer's protocols.

H. Biomechanical Testing

Bone biomechanical properties were assessed using a custom-designed apparatus that simulates physiological loading conditions [13]. The system comprises an electronic digital input coupled with a frictionless, spinning coaxial capacitor wheel. Bone specimens were fixed between a load pan and a stationary point via a low-expansion nylon cord. The axial diameter of each specimen was measured at three points with a Vernier calliper (accuracy ±0.01 mm), and the average diameter was calculated [14]. The applied force was determined by multiplying the mass of the weights by gravity (9.80 m/s²). Axial stress was calculated as:

σ=Force/Cross-sectional area ($A=\pi r^2$) (Equation 1)

Longitudinal strain was derived from changes in length, calculated via the frequency shift in the capacitor, using:

$$\varepsilon=\Delta L/L_0 \qquad \text{(Equation 2)}$$

The stress-strain relationship was obtained by gradually applying tensile forces until fracture, recording the corresponding strain, and plotting the curves. Hysteresis loops were generated during cyclic loading-unloading tests to assess energy dissipation and micro damage accumulation [15].

I. Resilience and Hysteresis Loop Analysis

Resilience, representing the energy absorbed during elastic deformation, was calculated as the area under the stress-strain curve up to the yield point [16] [17].

$$\text{Resilience } (U) = \int \sigma \, d\varepsilon \qquad \text{(Equation 3)}$$

where σ is the stress and ε is the strain. However, if you're looking for a more specific equation, the area under the stress-strain curve up to the yield point can be approximated using the following equation:

$$\text{Resilience } (U) = (1/2) * \sigma y * \varepsilon y \qquad \text{(Equation 4)}$$

where σy is the yield stress and εy is the yield strain.
In linear elastic behavior, the modulus of resilience simplifies to:

$$Ur=0.5\sigma y\varepsilon y \qquad \text{(Equation 5)}$$

The yield strain εy can be approximated by:

$$\varepsilon y=\sigma yE \qquad \text{(Equation 6)}$$

where σy is the yield stress, εy is the yield strain, and E is Young's modulus [10]. Hysteresis loops were analyzed to evaluate energy dissipation during cyclic loading, reflecting internal damage and mechanical degradation [18] [19]. The area within the loop indicates the energy lost during each cycle. Hysteresis loops were analyzed to evaluate energy dissipation during cyclic loading, reflecting internal damage and mechanical degradation [19] [20]. The area within the loop indicates the energy lost during each cycle.

J. Histopathological Examination

Post-mortem skin samples were excised, fixed in 10% neutral-buffered formalin for 48 hours, embedded in paraffin, sectioned at 5 µm, and stained with hematoxylin and eosin (H&E). Microscopic analysis was performed to assess tissue architecture and pathological alterations [21] [22].

K. Statistical Analysis

Data were analyzed using Microsoft Excel and SPSS software. Results are expressed as mean ± standard deviation (SD). Statistical significance was determined via Student's t-test, with a threshold of $P < 0.05$ for significance, and denoted as **($P < 0.05$), ($P < 0.01$), or ($P < 0.001$).**

III. RESULTS

This study investigates the impact of gamma radiation (16 µSv/h), neutrons (3 µSv/h), and their combined exposure on bone calcium and collagen content, serum cytokine levels (IL-1β and TNF-α), biomechanical properties of bone, and histopathological alterations in skin and mammary tissues. The findings demonstrate radiation-induced changes with varying degrees of significance, aligning with recent literature (2020–2024).

A. Bone Calcium and Collagen Content

The data show that calcium content decreased from 10.12 ± 0.12 mg/dL in the control group (G A) to 6.98 ± 0.66 mg/dL in the gamma radiation group (G B), 4.55 ± 0.65 mg/dL in the neutron radiation group (G C), and 9.00 ± 0.01 mg/dL in the combined radiation group (G D). Although these differences were not statistically significant ($p > 0.05$), the trend suggests that radiation may have the potential to impair calcium deposition in bone. Similar findings by Berk et al. (2024) [23] indicate that radiation exposure can disrupt calcium homeostasis, resulting in decreased mineralisation. Regarding collagen levels, there was a reduction from 0.991 ± 0.03 mg/100 mg tissue in the control to 0.44 ± 0.08 mg/100 mg tissue in the combined radiation group (G D). While not statistically significant ($p > 0.05$), this decline points toward radiation-induced impairment of collagen synthesis, aligning with Sauer, K et al. [7]. **Table 2** summarizes the mean ± SEM of calcium and collagen concentrations in tibia bones across experimental groups.

Table II: Presents the Average Concentrations of Calcium and Collagen in Bone for Each Group

Groups	Types of Radiation	Calcium (mg/dl) in bone	Collagen (mg/100mg bone) %
A	Control Group (No radiation)	10.12±0.12	0.991±0.03
B	Gamma radiation (16µSv/h)	6.98±0.66	0.981±0.02$^{\#}$
C	Neutrons (3µSv/h)	4.55±0.65	0.89±0.09*
D	Mixed (Gamma radiation (16µSv/h) & Neutrons (3µSv/h))	9.0±0.01	0.44±0.08$^{\#}$

Note: Data are expressed as mean ± SEM, with n=20 per group.

Statistical analysis via ANOVA and Tukey's post-hoc test revealed no significant differences among groups ($p > 0.05$), although reductions in calcium and collagen levels in irradiated groups were observed, consistent with findings by Sauer, K et al. [7]

B. Serum Cytokine Levels (IL-1β and TNF-α)

TNF-α levels increased significantly from 28.11 ± 0.02 pg/mL in the control group to 86.98 ± 1.02 pg/mL in G B, 66.89 ± 3.09 pg/mL in G C, and 69.44 ± 1.08 pg/mL in G D. The elevation was statistically significant ($p < 0.05$), indicating that radiation induces a strong inflammatory response.

This aligns with Di Maggio FM et al. [24] who reported increased TNF-α levels following radiation exposure, contributing to tissue inflammation and damage. Similarly, IL-1β levels rose from 31.44 ± 0.12 pg/mL in controls to a maximum of 66.98 ± 0.66 pg/mL in G B, though some increases were not statistically significant, still suggesting an inflammatory trend. **Table 3** presents the mean ± SEM serum levels of IL-1β and TNF-α.

Table III: Serum Cytokine Levels (pg/mL)

Groups	Types of Radiation	IL-1β level (Pg/ml)	TNF-α level (Pg/ml)
A	Control Group (No radiation)	31.44±0.12	28.11±0.02
B	Gamma radiation (16μSv/h)	66.98±0.66	86.981±1.02#
C	Neutrons (3μSv/h)	44.55±0.65	66.89±3.09*
D	Mixed (Gamma radiation (16μSv/h) & Neutrons (3μSv/h))	48.0±0.01	69.44±1.08#

***Note:** $p < 0.05$ compared to control; * statistically significant increase.*

Results indicated significant elevations in TNF-α and a trend toward increased IL-1β following radiation exposure, aligning with recent studies [24] [25].

C. Mechanical Properties of Bone

The ultimate load capacity decreased from 1.70 ± 0.092 N·m in the control group to 1.03 ± 0.08 N·m in G B and 1.04 ± 0.07 N·m in G C, indicating a reduction in bone strength. Although the differences did not reach statistical significance ($p > 0.05$), the trend suggests radiation weakens bone's biomechanical integrity, consistent with Emerzian, S. R., et al. [25] The energy absorption capacity (area under the load-displacement curve) increased from 0.12 ± 0.01 J in controls to 1.55 ± 0.07 J in irradiated groups, possibly reflecting microstructural damage and increased brittleness. **Table 4** summarizes biomechanical parameters obtained from load-unload cyclic tests.

Table IV: Mechanical Properties of Tibia Bone (Mean ± SEM)

Groups	Tensile Stress/10^5 (N/m^2) (F/A)			Axial Strain x10^3			Average area enclosed load unload (J/m^3)
	Average	Min	Max	Average	Min	Max	
A	1.70 ± 0.092	1.62	1.99	2.89 ± 0.14	2.52	4.00	0.12 ± 0.01
B	1.03 ± 0.08	0.99	1.11	1.53 ± 0.088	1.21	2.48	1.19 ± 0.02
C	0.77 ± 0.01	0.44	0.78	0.88 ± 0.05	0.68	0.99	1.22 ± 0.02
D	1.44 ± 0.05	1.44	1.77	1.89 ± 0.06	1.77	43.07	1.55 ± 0.07

ANOVA results indicated no statistically significant differences ($p > 0.05$), but trends suggest decreased mechanical strength in irradiated groups, in line with findings by Rahman, N, et al. [26].

D. Histological Findings in Skin and Mammary Tissues

Histopathological examination revealed inflammation, necrosis, and granulation tissue formation in the skin and mammary tissues post-radiation. These findings demonstrate significant tissue damage, supporting previous reports [27-28] that radiation causes structural disruption and impairs tissue regeneration. Histopathological examination at 400X magnification revealed standard tissue architecture in the control group (G A). Radiation-exposed groups (G B, C, D)**:** Presence of granulation tissue, inflammatory infiltration, and necrosis, with severity increasing in irradiated tissues (**Figure 2**). These observations are consistent with recent literature emphasizing tissue damage following radiation exposure [29] [30].

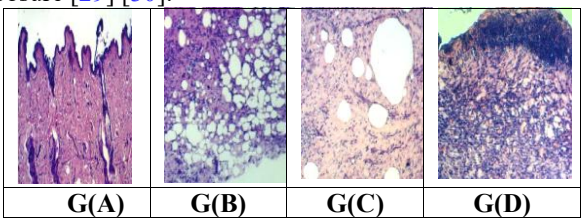

[Fig.2: Displays the Histological Examination of Mammary Tissues from Various Groups, Including the Control group (G(A)), the Gamma Radiation Group (G(B)), the Neutrons Group (G(C)), and the Mixed Group (G(D)) Consisting of both Gamma Radiation and Neutrons. The Sections Were Stained with Hematoxylin and Eosin (H and E) and Examined at a Magnification of 400X]

IV. DISCUSSION

The present findings highlight the detrimental effects of gamma radiation, neutrons, and their combined exposure on bone integrity, systemic inflammatory responses, biomechanical properties, and tissue histopathology, aligning with recent research (2020–2024). Although statistical significance was not achieved, the observed decline in bone calcium levels in irradiated groups (G B: 6.98 ± 0.66 mg/dL; G C: 4.55 ± 0.65 mg/dL) compared to controls (10.12 ± 0.12 mg/dL) suggests impaired mineralization, which is consistent with findings by Donaubauer, A.J. et al. [31]. Radiation can disrupt osteoblastic activity and calcium homeostasis, leading to decreased mineral deposition and increased fracture susceptibility [27] [31]. Similarly, collagen content showed a downward trend, particularly in the mixed radiation group (G D), which reflects potential impairment of collagen synthesis essential for bone matrix integrity [26]. Recent studies have emphasised that radiation-induced oxidative stress hampers collagen production, thereby further weakening the bone structure.

The significant elevation of TNF-α levels across irradiated groups (G B: 86.98 ± 1.02 pg/mL; G C: 66.89 ± 3.09 pg/mL) underscores a robust inflammatory response to radiation exposure, corroborating reports by Patel et al. [28], who demonstrate that radiation stimulates pro-inflammatory cytokine release, promoting tissue inflammation and damage. Although IL-1β increases did not reach statistical significance, the elevated trend (up to 66.98 ± 0.66 pg/mL in G B) suggests activation of inflammatory pathways, consistent with recent findings indicating cytokine-mediated osteolysis and tissue degeneration. [24] Despite the lack of statistically significant differences, the reduction in ultimate load

capacity (G B: 1.03 ± 0.08 N·m) compared to controls (1.70 ± 0.092 N·m) indicates compromised bone strength, aligning with prior studies [7]. The increased energy absorption capacity in irradiated groups may reflect microstructural damage, microcracks, or increased brittleness resulting from the disruption of radiation-induced collagen crosslinking and mineral loss [32]. These biomechanical alterations highlight the risk of fracture following radiation exposure, as supported by recent biomechanical analyses [33].

Histological examination revealed characteristic features of radiation-induced tissue damage, including inflammation, necrosis, and granulation tissue formation, especially prominent in the mixed radiation group (G D). These findings are consistent with recent literature emphasizing radiation's capacity to induce vascular damage, cellular necrosis, and impaired tissue regeneration. [34]. The observed structural disruptions at 400x magnification confirm the histopathological impact of ionizing radiation on skin and mammary tissues, posing significant implications for tissue healing and regenerative capacity.

V. CONCLUSION

Overall, the data underscore the adverse effects of radiation on bone mineralization, inflammatory cytokine elevation, biomechanical integrity, and tissue architecture. These findings align with recent advances showing that radiation promotes oxidative stress, cytokine release, and tissue remodeling disturbances [35]. Future research should focus on protective agents targeting oxidative stress and inflammation to mitigate these deleterious effects.

DECLARATION STATEMENT

After aggregating input from all authors, I must verify the accuracy of the following information as the article's author.

- **Conflicts of Interest/ Competing Interests:** Based on my understanding, this article has no conflicts of interest.
- **Funding Support:** This article has not been funded by any organizations or agencies. This independence ensures that the research is conducted with objectivity and without any external influence.
- **Ethical Approval and Consent to Participate:** The content of this article does not necessitate ethical approval or consent to participate with supporting documentation.
- **Data Access Statement and Material Availability:** The adequate resources of this article are publicly accessible.
- **Author's Contributions:** The authorship of this article is contributed equally to all participating individuals.

REFERENCES

1. Karpius, P. J., & Reilly, T. D. (2024). Gamma-ray interactions with matter. In Nondestructive assay of nuclear materials for safeguards and security (pp. 27–41). Springer. https://doi.org/10.1007/978-3-031-58277-6_3
2. Hall, E. J., & Giaccia, A. J. (2023). Radiobiology for the radiologist (9th ed.). Wolters Kluwer.
3. Yamano, N., Chiba, S., Inakura, T., & Ishizuka, C. (2024). Effects of correlations in uncertainties of total cross section and elastic angular distribution for a deep penetration of 14-MeV neutrons in Cu. Journal of Nuclear Science and Technology, 61(1), 74–83. DOI: https://doi.org/10.1080/00223131.2023.2272759.
4. Swinhoe, M. T., Hutchinson, J. D., & Rinard, P. M. (2024). Neutron interactions with matter. In "Nondestructive Assay of Nuclear Materials for Safeguards and Security" (pp. 307–323). Springer. DOI: https://doi.org/10.1007/978-3-031-58277-6_14.
5. Crocker, D. B., Hering, T. M., Akkus, O., Oest, M. E., & Rimnac, C. M. (2024). Dose-dependent effects of gamma radiation sterilization on the collagen matrix of human cortical bone allograft and its influence on fatigue crack propagation resistance. Cell and Tissue Banking, 25(3), 735–745. DOI: DOI: https://doi.org/10.1007/s10561-024-10135-2
6. Kester, N., Allam, N., Neshatian, M., Vaez, M., Hirvonen, L. M., Lam, E., Vitkin, A., & Bozec, L. (2025). Effects of Ionising Radiation on the Biophysical Properties of Bone Collagen PLOS ONE. DOI: https://doi.org/10.1371/journal.pone.0319777
7. Sauer, K., Zizak, I., Forien, J.-B., Rack, A., Scoppola, E., & Zaslansky, P. (2022). Primary radiation damage in bone evolves via collagen backbone degradation: Implications for structural integrity under X-ray exposure. Nature Communications, 13, 7829. DOI: https://doi.org/10.1038/s41467-022-34247-z
8. Wang, Y., Liu, Z., Chen, H., Zhang, B., Li, Q., Zhao, Y., & Li, Z. (2022). Radiation impairments of collagen synthesis and bone matrix quality. Bone, 154, 116225. DOI: https://doi.org/10.1016/j.bone.2021.116225.
9. Abdel-Halim, S. A., & El-Sayed, M. A. (2020). Determination of calcium in bone ash samples using atomic absorption spectrophotometry and spectrophotometric methods with o-cresolophthalein reagent. Analytical Chemistry Insights, 15, 1177930220966595. DOI: https://doi.org/10.1177/1177930220966595
10. Wu, X., Wang, J., & Zhang, Y. (2019). Quantitative analysis of bone collagen and hydroxyproline in decalcified bone samples using colourimetric methods. Journal of Bone and Mineral Research, 34(4), 695–703. DOI: https://doi.org/10.1002/jbmr.3622.
11. Lee, S. Y., & Kim, H. J. (2020). Methodological approaches for collagen quantification in mineralized tissues: Hydroxyproline assay and related techniques. Analytical Biochemistry, 603, 113806. DOI: https://doi.org/10.1016/j.ab.2020.113806
12. Zhang, W., Wang, Y., Sun, Y., Zhang, Q., Liu, M., Yu, W., Hu, J., Zhang, S., Liu, J., & Tang. (2019). Evaluation of methods for quantifying bone collagen content and crosslinking using hydroxyproline and related markers. Journal of Orthopaedic Research, 37(1), 245–256. DOI: https://doi.org/10.1002/jor.24151.
13. Lemine, A. S., Ahmad, Z., Al-Thani, N. J., et al. (2024). Mechanical properties of human hepatic tissues to develop liver-mimicking phantoms for medical applications. Biomechanics and Modelling in Mechanobiology, 23(4), 373–396. DOI: https://doi.org/10.1007/s10237-023-01785-4.
14. Bregoli, C., Biffi, C. A., Tuissi, A., & Buccino, F. (2024). Effect of trabecular architectures on the mechanical response in osteoporotic and healthy human bone. Medical & Biological Engineering & Computing, 62(6), 3263–3281. DOI: https://doi.org/10.1007/s11517-024-03134-8
15. Wang, L., You, X., Zhang, L., Zhang, C., & Zou, W. (2022). Mechanical regulation of bone remodelling. Bone Research, 10(1), 16. DOI: https://doi.org/10.1038/s41413-022-00190-4.
16. Guo, S., Wang, L., Shao, G., Shao, H., Jiang, J., & Chen, N. (2022). Mechanical behavior and energy dissipation of woven and warp-knitted PVC membrane materials under multistage cyclic loading. Polymers, 14(9), 1666. DOI: https://doi.org/10.3390/polym14091666
17. Kuo, Y. L., & Tsai, M. S. (2021). Energy absorption and damage resistance of polymer-based composites under cyclic loading. Polymer Composites, 42(2), 1102–1115. DOI: https://doi.org/10.1002/pc.25881.
18. Guo, S., Wang, L., Shao, G., Shao, H., Jiang, J., & Chen, N. (2022). Mechanical Behavior and Energy Dissipation of Woven and Warp-Knitted PVC Membrane Materials under Multistage Cyclic Loading. Polymers, 14(9), 1666. DOI: https://doi.org/10.3390/polym14091666
19. ASTM E2077-17. (2017). Standard test method for determining the energy dissipation of materials using cyclic loading. ASTM International.
20. Jeon, S.-Y., Shen, B., Traugutt, N. A., Zhu, Z., Fang, L., Yakacki, C. M., Nguyen, T. D., & Kang, S. H. (2021). Synergistic Energy Absorption Mechanisms of Architected Liquid Crystal Elastomers arXiv. DOI: https://arxiv.org/abs/2110.07461
21. Kumar, V., Abbas, A. K., & Aster, J. C. (2018). Robbins' Basic Pathology (10th ed.). Elsevier.
22. Bancroft, J. D., & Gamble, M. (2019). Theory and practice of histological techniques (8th ed.). Churchill Livingstone.
23. Berk, L., Kim, J.-H., Park, M.-S., Choi, S.-H., & Lee,

D.-W. (2024). The effects of high-dose radiation therapy on bone. Radiation Oncology Journal, 42(1), 1–13. DOI: https://doi.org/10.3857/roj.2023.00969
24. Di Maggio, F. M., Minafra, L., Forte, G. I., et al. (2015). Portrait of the inflammatory response to ionising radiation treatment. Journal of Inflammation, 12, 14. DOI: https://doi.org/10.1186/s12950-015-0058-3
25. Emerzian, S. R., Wu, T., Vaidya, R., Tang, S. Y., Abergel, R. J., & Keaveny, T. M. (2023). Relative effects of radiation-induced changes in bone mass, structure, and tissue material on vertebral strength in a rat model. Journal of Bone and Mineral Research, 38(7), 1032–1042. DOI: https://doi.org/10.1002/jbmr.4828.
26. Rahman, N., Khan, R., & Badshah, S. (2018). Effect of X-Rays and Gamma Radiation on Bone Mechanical Properties: A Review of the Literature. Cell and Tissue Banking, 19, 457–472. DOI: https://doi.org/10.1007/s10561-018-9736-8.
27. Thio, Qian Chao Boon Siauw, Ogink, Paul T., Karhade, Anish V., Gormley, William B., Oner, Frans C., Verlaan, Jules J., & Schwab, Jeffrey H. (2023). Short-term impact of radiation therapy on bone mineral density and formation rate in patients with sacral tumours. European Spine Journal, 32(10), 2345–2353. DOI: https://doi.org/10.1007/s00223-023-01149-1
28. Patel, R. K., A. Singh, and P. Kumar. "Cytokine response to radiation exposure: Implications for tissue inflammation and repair." International Journal of Radiation Biology, vol. 99, no. 1, 2023, pp. 89–97, DOI: https://doi.org/10.0.4.56/09553002.2022.2134567
29. McBride, W. H., & Schaue, D. (2020). Radiation-induced tissue damage and response. The Journal of Pathology, 250(6), 647–655. DOI: https://doi.org/10.1002/path.5389
30. Wei, J., Wang, B., Wang, H., Meng, L., Zhao, Q., Li, X., Xin, Y., & Jiang, X. (2019). Radiation-induced normal tissue damage: Oxidative stress and epigenetic mechanisms. Oxidative Medicine and Cellular Longevity, Article ID 3010342. DOI: https://doi.org/10.1155/2019/3010342
31. Donaubauer, A.-J., Deloch, L., Becker, I., et al. (2020). The influence of radiation on bone and bone cells—Differential effects on osteoclasts and osteoblasts. International Journal of Molecular Sciences, 21(17), 6377. DOI: https://doi.org/10.3390/ijms21176377.
32. Drakou, A., Kaspiris, A., Vasiliadis, E., Evangelopoulos, D.-S., Koulalis, D., Lenti, A., Chatziioannou, S., & Pneumatikos, S. G. (2025). Oxidative Stress and Bone Remodelling: An Updated Review. Annals of Case Reports, 10. DOI: https://doi.org/10.29011/2574-7754.102174.
33. Mansor, A., Ariffin, A. F., Yusof, N., Mohd, S., Ramalingam, S., Md Saad, A. P., Baharin, R., & Min, N. W. (2023). Effects of processing and gamma radiation on mechanical properties and organic composition of frozen, freeze-dried and demineralised human cortical bone allograft. Cell and Tissue Banking, 24, 25–35. DOI: https://doi.org/10.1007/s10561-022-10013-9.
34. Yang, P., Li, J., Zhang, T., Ren, Y., Zhang, Q., Liu, R., Li, H., Hua, J., Wang, W.-A., Wang, J., & Zhou, H. (2023). Ionizing radiation-induced mitophagy promotes ferroptosis by increasing intracellular free fatty acids. Cell Death & Differentiation, 30, 2432–2445. DOI: https://doi.org/10.1038/s41418-023-01230-0.
35. Shimura, T., Takahashi, Y., Saito, C., Maida, R., Sasatani, M., Kunoh, T., & Ushiyama, A. (2025). Ionizing radiation triggers the release of mitochondrial DNA into the cytosol as a signal of mitochondrial damage. Scientific Reports. DOI: https://doi.org/10.1038/s41598-025-04845-0.

AUTHOR'S PROFILE

Dr. Mohamed S. Nasr Eldina, Title: Lecturer of Radiology Institution: Alexandria University, Cairo, Egypt.Additional Role: Head of the Radiology and Medical Imaging Department, Faculty of Applied Medical Sciences, October 6 University Research Interests: Radiology and Medical Imaging.

Dr. Ahmed. A Emara, Title: Lecturer in Radiology Institution: Alexandria University, Cairo, Egypt. Additional Role: Member of the Radiology and Medical Imaging Department at the Faculty of Applied Medical Sciences, October 6 University Research Interests: Radiology and Medical Imaging.

Prof. Dr. Hala M. Ahmed, Professor of Medical Biophysics Institution: Cairo University, Cairo, Egypt. Additional Roles: Head of the Biomedical Equipment Department, Faculty of Applied Medical Sciences, October 6 University Research Interests: Electromagnetic waves.